A silicon-nanowire memory driven by optical gradient force induced bistability

Yang, Z. C.; Gu, Y. D.; Ng, Geok Ing; Ser, Wee; Kwong, D. L.; Dong, Bin; Cai, H.; Chin, Lip Ket; Huang, Jianguo; Liu, Ai Qun

2015

Dong, B., Cai, H., Chin, L. K., Huang, J. G., Yang, Z. C., Gu, Y. D., et al. (2015). A silicon-nanowire memory driven by optical gradient force induced bistability. Applied Physics Letters, 107(26), 261111-.

https://hdl.handle.net/10356/82448

https://doi.org/10.1063/1.4939114

A silicon-nanowire memory driven by optical gradient force induced bistability

B. Dong, H. Cai, L. K. Chin, J. G. Huang, Z. C. Yang, Y. D. Gu, G. I. Ng, W. Ser, D. L. Kwong, and A. Q. Liu

Citation: Applied Physics Letters **107**, 261111 (2015); doi: 10.1063/1.4939114
View online: http://dx.doi.org/10.1063/1.4939114
View Table of Contents: http://scitation.aip.org/content/aip/journal/apl/107/26?ver=pdfcov
Published by the AIP Publishing

A silicon-nanowire memory driven by optical gradient force induced bistability

B. Dong,[1,2] H. Cai,[2,a)] L. K. Chin,[1] J. G. Huang,[1,2,3] Z. C. Yang,[4] Y. D. Gu,[2] G. I. Ng,[1] W. Ser,[1] D. L. Kwong,[2] and A. Q. Liu[1,4,b)]
[1]*School of Electrical and Electronic Engineering, Nanyang Technological University, Singapore 639798*
[2]*Institute of Microelectronics, A*STAR (Agency for Science, Technology and Research), Singapore 117685*
[3]*School of Mechanical Engineering, Xi'an Jiaotong University, Xi'an 710049, China*
[4]*School of Electronics Engineering and Computer Science, Peking University, Beijing 100871, China*

(Received 21 October 2015; accepted 15 December 2015; published online 30 December 2015)

In this paper, a bistable optical-driven silicon-nanowire memory is demonstrated, which employs ring resonator to generate optical gradient force over a doubly clamped silicon-nanowire. Two stable deformation positions of a doubly clamped silicon-nanowire represent two memory states ("0" and "1") and can be set/reset by modulating the light intensity (<3 mW) based on the optical force induced bistability. The time response of the optical-driven memory is less than 250 ns. It has applications in the fields of all optical communication, quantum computing, and optomechanical circuits. © *2015 AIP Publishing LLC*. [http://dx.doi.org/10.1063/1.4939114]

Either all-optical or quantum computing has long been seen as candidates to replace current electronic computing due to the advantages such as high speed and high bandwidth.[1,2] But the lack of memory has been one obstacle that hinder the development of all-optical and quantum computing. All optical memory based on microring laser was developed using group II/V materials,[3] which is not CMOS compatible and costly, hindering its capability for photonic circuit integration. On the other hand, mechanical memory recently draws more attention due to the advantage of high speed. For example, MEMS memory can work at faster speed (microsecond level) compared with conventional non-volatile memory (1–5 ms).[4] Therefore, optomechanical switching and memory elements are in great demands for all-optical signal buffering of decisions and telecommunication data in the current high speed and high capacity applications such as all-optical and quantum computing and fiber optics telecommunication systems.[3,5]

Currently, most memories are based on either mechanical bistability[6–12] or material-based bistability[13] to meet the requirements of compactness and high speed. However, current approaches either require special materials, such as magnetic materials as highly nonlinear optical materials, or complex electrostatic force actuated mechanical structures, which typically are bulky, slow, and power inefficient. Recently, non-volatile mechanical memories based on nano-mechanical resonators have been reported, which rely on the mechanical bistability of a silicon-nanowire driven by an optical gradient force.[14] Optical gradient force has been exploited for amplification, cooling, and actuation of nano-scale devices.[15–17] However, the non-linearity of optical gradient force hedges its further development. In this paper, the non-linearity of optical gradient force is utilized to realize bistability through optical signal modulation. Such optical gradient force induced bistability can be used to realize switching effects, working as an element of optical memory. A silicon-nanowire memory based on optomechanical effect has a great potential in optical signal buffering, switching, and processing on silicon photonic circuits due to its high speed, compact size, and high integrability.

The basic element of the silicon-nanowire memory consists of a ring resonator, a doubly clamped silicon-nanowire, and a bus waveguide, as shown in Figure 1(a). The operation

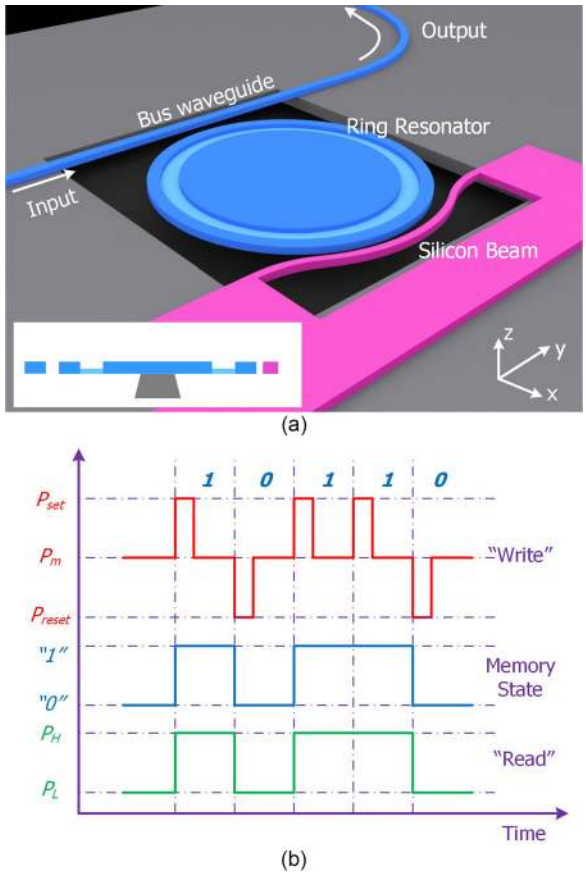

FIG. 1. (a) Schematic illustration and (b) operation principle of the silicon-nanowire optomechanical memory element.

a)Email: caih@ime.a-star.edu.sg
b)Email: eaqliu@ntu.edu.sg

of the silicon-nanowire memory element requires two lights to realize the write and read processes, named WRITE (W) light and READ (R) light. The W light is coupled from the bus waveguide into the ring resonator and the optical gradient force is thereafter initiated between the ring resonator and the silicon nanowire. Such force pulls the silicon nanowire towards the ring resonator. The silicon nanowire has two stable positions owing to the nonlinearity of the optical gradient force, which are identified as memory states. These memory states are thereafter identified as different intensity levels of the R light. The operation of the optomechanical memory is summarized in Figure 1(b). The W light can set the memory to "1" with a high power pulse (P_{set}) with the transmission of the R light being kept at high power level (P_H). Otherwise, the W light can reset the memory to "0" with the notch in power (P_{reset}) such that the transmission of the R light is kept at low power level (P_L).

The wavelength of W light λ_W is red detuned as compared with the resonance wavelength of the ring resonator and the wavelength detuning is defined as

$$\delta = \lambda_W - \lambda(0), \tag{1}$$

where $\lambda(0)$ is the resonance wavelength of the ring resonator at zero deformation. The resonance wavelength of ring resonator depends on the geometry of the ring resonator, which is defined as

$$\lambda = \frac{2\pi n_{eff} R}{N}, \tag{2}$$

where R is the radius of the ring resonator and N is an integral number. The effective refractive index n_{eff} describes the light propagation properties in waveguides and can be simulated by using Lumerical. The generated optical gradient force by W light can be expressed as[18]

$$F_{optical}(x) = -\frac{2\gamma_e P_{optical}}{n_{eff}(x)} \frac{g_{om}(x)}{\Delta(x)^2 + \gamma^2}, \tag{3}$$

where γ_e is the external damping due to waveguide-ring coupling, $P_{optical}$ is the light power, $g_{om}(x)$ is the optomechanical coupling coefficient, γ is the total damping coefficient, and $\Delta(x)$ is the laser detuning that is defined as

$$\Delta(x) = \omega(x) - \omega_W = 2\pi c \left[\frac{1}{\lambda(x)} - \frac{1}{\lambda_W}\right], \tag{4}$$

where $\lambda(x)$ is the resonance wavelength of the ring resonator at x deformation of the silicon nanowire.

The optical gradient force is balanced by the mechanical restoring force, which "pulls" the nanowire back to its original position. The mechanical restoring force increases linearly as the deformation of the silicon-nanowire increases as shown in Figure 2(a) and the slope is the mechanical spring constant, which is simulated by using COMSOL Multiphysics. The curves have several intersections, which stand for stable positions of the silicon-nanowire. When the light power is 1 mW, there is only one cross-point (named "A"), which is the only stable position and the deformation of the silicon-nanowire is approximately 2.48 nm. When the light power is increased to

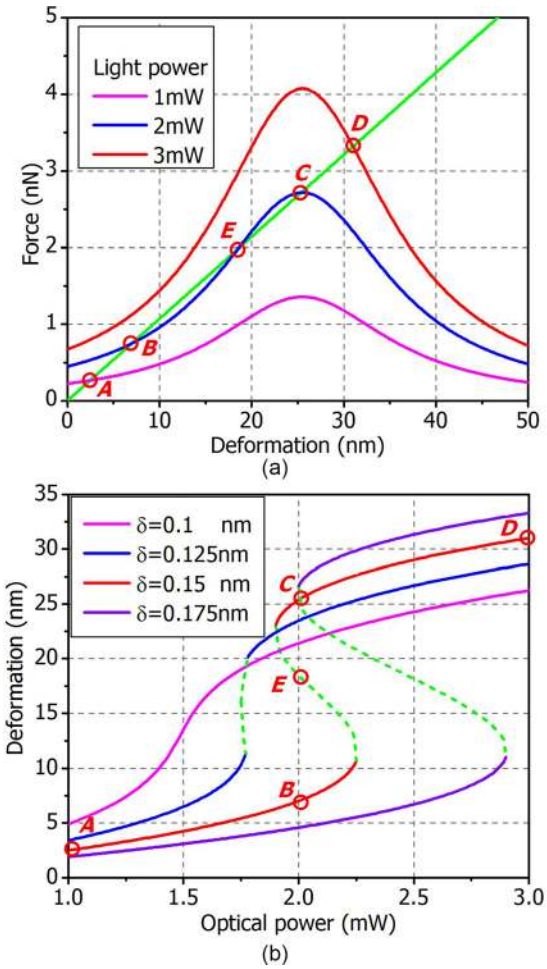

FIG. 2. (a) Optical gradient force when the wavelength detuning is $\delta = 0.15$ nm and mechanical restoring force over the silicon-nanowire, and (b) simulated deformation of silicon-nanowire versus optical power with different wavelength detunings.

3 mW, there is one cross-point (named "D"), which is also the only stable position with 30.9-nm deformation of the silicon-nanowire. When the light power is 2 mW, there are three cross-points, and two of them (named "B" and "C") are in stable positions. The "E" is not stable because a small disturbance can induce a net force whose direction is towards either "B" or "C." Therefore, the silicon-nanowire can rest at either position when the WRITE light is at 2 mW, corresponding to 6.9 nm ("B") or 25.3 nm ("C") deformation. By tuning the light power, the silicon-nanowire can be transferred between the two stable deformations. The bistable hysteresis curve at 0.15-nm wavelength detuning is calculated and is shown in Figure 2(b). The deformation of the silicon-nanowire increases from 0 to 10.7 nm, while the optical power increases from 0 to 2.25 mW. When the optical power increases further, the deformation of the silicon-nanowire "jumps" to 27.5 nm and increases further as power increases. When the power decreases from 3 to 1.9 mW, the deformation decreases continuously to 23.1 nm. By further decreasing the power, another abrupt change in the deformation is induced, which is from 23.1 nm to 6.3 nm.

The silicon-nanowire shows bistability when it is deformed by the optical gradient force. Such bistability is not due to the mechanical properties of the silicon-nanowire,

but can be manipulated by controlling the wavelength and power of the W light, as shown in Figure 2(b). The silicon-nanowire is deformed in different paths based on different wavelength detunings. When the wavelength detuning is 0.1 nm, the silicon-nanowire shows only one stable position at all times and therefore no bistability. When the wavelength detuning is increased to 0.125 nm, there is only a very narrow region where the silicon-nanowire shows two stable positions and the transition curve is close to a vertical line. This is the critical condition where the silicon-nanowire starts to show bistability. When the wavelength detuning is increased to 0.175 nm, the bistable region is further broadened. Therefore, both the power and wavelength of write light are critical to control the bistability of the silicon-nanowire.

The deformations of the silicon-nanowire are sensed by the R light. Initially, the wavelength of the R light matches with another resonance wavelength of the ring resonator, causing a low power level (P_L) at output. When the power of the W light is increased, the optical gradient force is increased and the silicon-nanowire moves towards the ring resonator. The deformation of the silicon-nanowire results in the change in the effective refractive index Δn_{eff} of the ring resonator, causing a red shift of the ring resonance wavelength $\Delta\lambda_r$. The R light can be transmitted through the waveguide, causing a high power level (P_H) at output, since its wavelength is no longer matched with the resonance wavelength now. Therefore, the transmission of the R light can be controlled by pumping a red-detuned W light powered at different levels.

The memory elements are connected together by the bus waveguides to form the memory array. Each element can be written and read individually by differentiating the resonance wavelength of each element. A 4×4 memory array, which integrates 16 memory elements, is fabricated by nano-silicon-photonic fabrication processes. Figure 3 shows the scanning electron microscope (SEM) image of the optomechanical memory array and the memory element. The waveguide structures have a width of 450 nm and a height of 220 nm for a single mode transmission. The silicon-nanowire is designed to have a width of 200 nm and is clamped by two anchors. The coupling gap between the ring resonator and the silicon-nanowire is 150 nm. The ring resonator has a diameter of 40 μm and is supported by a rib structure and released from the substrate. The rib structure is only 80 nm in thickness such that it has negligible influence over the light propagating in the ring resonator while providing mechanical support to the ring resonator. The waveguides and ring resonators are patterned by deep UV lithography and followed by plasma dry etching. After etching, a 2-μm SiO_2 layer is deposited on the structure layers to ensure a low optical loss. A 40-nm Al_2O_3 is deposited and patterned, which is used as the protection film to protect those fixed structures during later HF vapor release due to its good mechanical stiffness, leaving an opening window area for suspended structures. Finally, HF vapor selectively undercuts the buried oxide layer in the window area to release the movable structures.

In the experiment, the W light is generated by a tunable laser source (Santec TCL510) and amplified by EDFA (Amonics EDFA-CL-27) before combining with the READ light from another tunable laser source through an optical coupler. The combined light is coupled to the bus waveguide

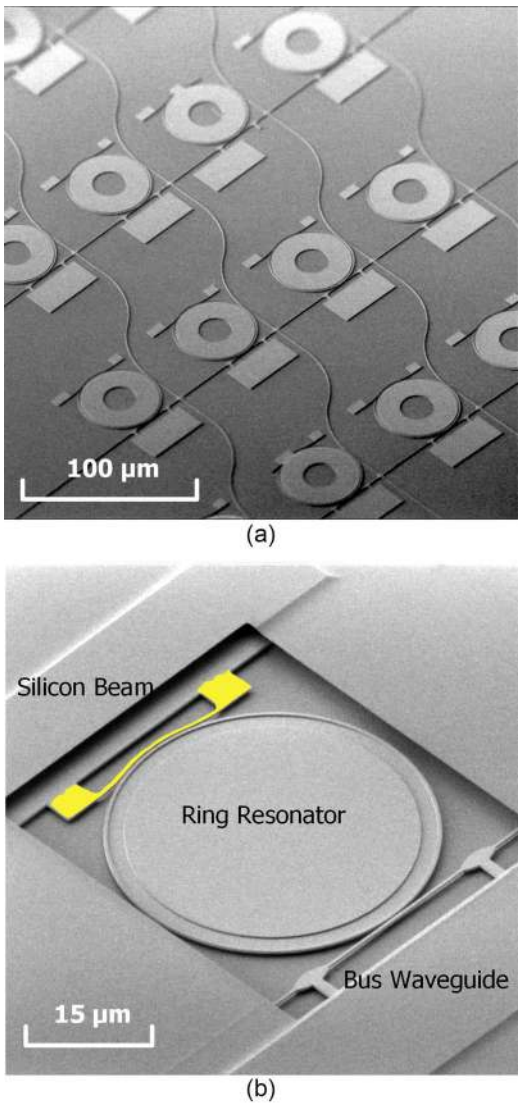

FIG. 3. SEM images of (a) 4×4 optomechanical memory array and (b) memory element.

through a tapered fiber. After passing through the device, the light is detected by an optical spectrum analyzer (Yokogawa AQ6370C) to monitor the transmission spectra. The power of WRITE light is modulated by tuning the pumping current of the EDFA. The transmission of the READ light is recorded by a high-speed photodetector (Menlo Systems FPD510).

The bistability of the optomechanical memory is experimentally verified by recording the resonance wavelength shift of the ring resonator at various W light, as shown in Figure 4(a). The wavelength detuning of the W light is 0.25 nm. When the power increases from 1 to 6 mW, the wavelength shift is less than 0.05 nm. The turning point is close to 6 mW, whereby the wavelength shift jumps from 0.05 to 0.38 nm. The wavelength shift reduces to 0.275 nm when the power is decreased to 2.1 mW. Then, the wavelength shift jumps back to 0.02 nm only when the power is further reduced.

The transmission spectra of the optomechanical memory element are recorded and are shown in Figure 4(b). The power of the red detuned (0.25 nm) W light is modulated among P_{set}, P_m, and P_{reset}. Initially, the power level is P_m

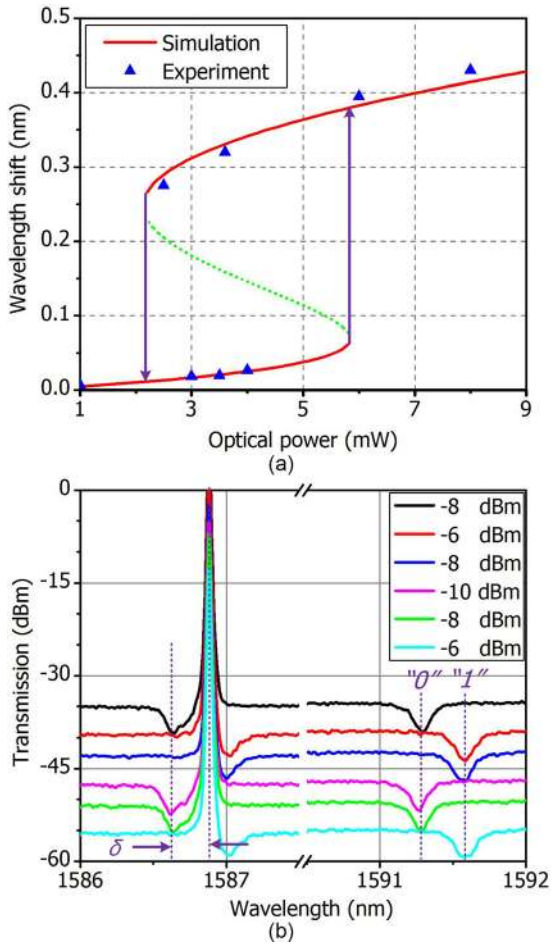

FIG. 4. (a) Simulation and experimental demonstration of optical force induced bistability and (b) transmission spectrum of the ring resonator versus write light when the wavelength detuning is 0.25 nm.

(−8 dBm, the black line), the resonance wavelength is close to 1593 nm, which is also the wavelength of the R light, the transmission of the R light is low, and the memory is at "0" state. When the power level is increased to P_{set} (−6 dBm, the red line), the resonance wavelength shifts to 1591.6 nm, the transmission of the R light is high and the memory is at "1" state. After the power level is decreased to P_m again (the blue line), the resonance wavelength maintains its current position with negligible blue shift, and the memory remain at "1." When the power is further reduced to P_{reset} (−10 dBm, the pink line), the resonance wavelength reduces to the original position, and the memory state is switched to "0." The memory state remains at "0" when the power is changed to P_m (the green line) again. Therefore, the intensity difference of the R light between "0" and "1" is approximately 4.7 dB. The time response of the optomechanical memory is also tested. The rise time is 243 ns while the fall time is 230 ns, as shown in Figure 5. The switching speed is restricted by the mechanical movement of the silicon-nanowire. The bistable optical-driven silicon-nanowire memory is fully functional throughout the experiment cycle, which lasts for 3 months. Furthermore, silicon material and devices are commonly known for their performance of high stability and reliability.[19]

In conclusion, a silicon-nanowire optomechanical memory was experimentally demonstrated. The silicon-nanowire

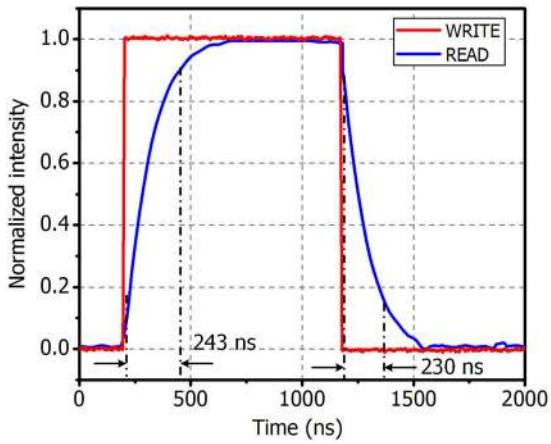

FIG. 5. Time response of the optomechanical memory.

memory is driven by the evanescent wave coupled optical gradient force. Two stable positions of the silicon-nanowire can be switched by pumping light with different power levels due to the optical force-induced bistability. The silicon-nanowire memory has advantages of small dimensions, low power consumption, easy integration, and fast response time with high potential for applications of on-chip all optical, quantum-computing, and fiber optical telecommunications.

The work was supported the Singapore Ministry of Education (MOE) (Grant No. RG 89/13).

[1]J. L. O'Brien, "Optical quantum computing," Science **318**(5856), 1567–1570 (2007).
[2]V. R. Almeida, C. A. Barrios, R. R. Panepucci, and M. Lipson, "All-optical control of light on a silicon chip," Nature **431**, 1081–1084 (2004).
[3]M. T. Hill, H. J. S. Dorren, T. de Vries, X. J. M. Leijtens, J. H. den Besten, B. Smalbrugge, Y.-S. Oei, H. Binsma, G.-D. Khoe, and M. K. Smit, "A fast low-power optical memory based on coupled micro-ring lasers," Nature **432**(7014), 206–209 (2004).
[4]A. Q. Liu, A. B. Yu, M. F. Karim, and M. Tang, "RF MEMS switches and integrated switching circuit," J. Semicond. Technol. Sci. **7**(3), 166–176 (2007).
[5]S. Zimmermann, A. Wixforth, J. P. Kotthaus, W. Wegscheider, and M. Bichler, "A semiconductor-based photonic memory cell," Science **283**(5406), 1292–1295 (1999).
[6]M. Hoffmann, P. Kopka, and E. Voges, "Bistable micromechanical fibre-optic switches on silicon with thermal actuators," Sens. Actuators, A **78**(1), 28–35 (1999).
[7]D. A. Tuan, K. G. Jayaraman, V. Pott, G. L. Chua, P. Singh, K. S. Yeo, and T. T. Kim, in 2013 IEEE International Symposium on Circuits and Systems (ISCAS), 2013.
[8]B. Halg, "On a micro-electro-mechanical nonvolatile memory cell," IEEE Trans. Electron Devices **37**(10), 2230–2236 (1990).
[9]J. Jeon, W. Kwong, and T. K. Liu, "Embedded memory capability of four-terminal relay technology," IEEE Trans. Electron Devices **58**(3), 891–894 (2011).
[10]W. Kwong, J. Jeon, L. Hutin, and T. K. Liu, "Electromechanical diode cell for cross-point nonvolatile memory arrays," IEEE Electron Device Lett. **33**(2), 131–133 (2012).
[11]V. Intaraprasonk, "Nonvolatile bistable all-optical switch from mechanical buckling," Appl. Phys. Lett. **98**(24), 241104 (2011).
[12]A. Uranga, J. Verd, E. Marigó, J. Giner, J. L. Muñóz-Gamarra, and N. Barniol, "Exploitation of non-linearities in CMOS-NEMS electrostatic resonators for mechanical memories," Sens. Actuators, A **197**, 88–95 (2013).
[13]G. Stegeman and E. Wright, "All-optical waveguide switching," Opt. Quantum Electron. **22**(2), 95–122 (1990).
[14]M. Bagheri, M. Poot, M. Li, W. P. H. Pernice, and H. X. Tang, "Dynamic manipulation of nanomechanical resonators in the high-amplitude regime and non-volatile mechanical memory operation," Nat. Nanotechnol. **6**(11), 726–732 (2011).

[15]H. Cai, K. J. Xu, A. Q. Liu, Q. Fang, M. B. Yu, G. Q. Lo, and D. L. Kwong, "Nano-opto-mechanical actuator driven by gradient optical force," Appl. Phys. Lett. **100**, 013108 (2012).
[16]T. J. Kippenberg and K. J. Vahala, "Cavity optomechanics: Back-action at the mesoscale," Science **321**(5893), 1172–1176 (2008).
[17]B. Dong, H. Cai, G. I. Ng, P. Kropelnicki, J. M. Tsai, A. B. Randles, M. Tang, Y. D. Gu, Z. G. Suo, and A. Q. Liu, "A nanoelectromechanical systems actuator driven and controlled by Q-factor attenuation of ring resonator," Appl. Phys. Lett. **103**, 181105 (2013).
[18]M. Ren, J. Huang, H. Cai, J. M. Tsai, J. Zhou, Z. Liu, Z. Suo, and A. Q. Liu, "Nano-optomechanical actuator and pull-back instability," ACS Nano **7**(2), 1676–1681 (2013).
[19]V. Lindroos, M. Tilli, A. Lehto, and T. Motooka, *Handbook of Silicon Based MEMS Materials and Technologies* (William Andrew Publishing, 2010).